On the Influence of a Lower Layer on the Propagation of Nonlinear Oceanic Eddies

ERIC P. CHASSIGNET*

National Center for Atmospheric Research, Boulder, Colorado

BENOIT CUSHMAN-ROISIN

Thayer School of Engineering, Dartmouth College, Hanover, New Hampshire

(Manuscript received 29 January 1990, in final form 11 January 1991)

ABSTRACT

The one-layer, reduced-gravity, also called equivalent-barotropic, model has been widely used in countless applications. Although its validity is based on the assumption that a second, lower layer is sufficiently deep to be dynamically inactive, the question of how deep that second layer ought to be has not yet received thorough examination. When one considers the importance of the two processes excluded from the reduced-gravity model, namely barotropic motion and baroclinic instability, the conventional choice of a second layer much deeper than the first might be too simplistic.

A scaling analysis aimed at covering all two-layer regimes, geostrophic as well as ageostrophic, leads to a double criterion, requiring that the total depth of fluid be much larger than either of two values. These values, resulting from f-plane and β-plane dynamics, apply to the shorter and longer scales, respectively. A number of numerical experiments on the propagation of eddies on the β-plane with various eddy radii and lower-layer depths verify the applicability of the criterion. A final set of experiments with dipoles on the f-plane and β-plane also clearly illustrates the two sides of the criterion.

The rule for the validity of the reduced-gravity model can be summarized as follows. For characteristic horizontal length scales of motion (e.g., eddy radius, wavelength, . . .) up to the deformation radius, it is sufficient that the lower layer be much deeper (e.g., by a factor ten or so) than the upper layer. For length scales increasing beyond the deformation radius, on both the f- and β-planes, the reduced-gravity model rapidly loses its validity. The model recovers its validity toward larger scales on the β-plane.

1. Introduction

Rings, i.e., oceanic eddies with a scale of a few hundred kilometers that detach from intense western boundary currents, represent one of the most energetic components of the world ocean mesoscale eddy field (Olson et al. 1985; Olson and Evans 1986). The role that these energetic features play in the general circulation is thought to be significant. In particular, by virtue of their formation process, eddies represent an efficient mechanism by which heat, salt and potential vorticity are transferred across frontal zones, which otherwise act as barriers to mixing between different water masses. In order to understand fully their importance on the world ocean circulation, however, it is helpful first to examine their behavior in isolation. In this study, rings are isolated in the sense that they are studied in the absence of boundaries and external shear, but are allowed to interact with the surrounding fluid. In most previous numerical works, the temporal evolution of isolated rings has been described in the framework of a particular approximation such as quasi-geostrophic (QG), reduced-gravity (1½ layer) or generalized geostrophic dynamics (Flierl 1977; McWilliams and Flierl 1979; Nof 1981, 1983a; Smith and Reid 1982; Davey and Killworth 1984; Cushman-Roisin and Tang 1990). For a review of works on isolated eddies on a β-plane, the reader is referred to Flierl (1987) and McWilliams (1991).

The problem associated with QG dynamics is well described by Flierl (1984) who states that "one of the serious flaws in the standard quasi-geostrophic equations, commonly used for understanding the evolution of mesoscale eddies, is the requirement that the change of thickness between density surfaces must be small compared to the mean thickness. In the case of warm-core rings, the thickness of the thermostads may vary from 500 m at the center to zero at the edge." The departure from QG dynamics in the ring behavior has been explored in some detail by McWilliams et al. (1986) using a balance-equation model (Norton et al. 1986). The standard was the more general and more

* Present address: RSMAS/MPO, University of Miami, Miami, Florida

Corresponding author address: Dr. Eric P. Chassignet, RSMAS, MPO, University of Miami, 4600 Rickenbacker Causeway, Miami, FL 33149.

complex primitive equations. The second approximation widely used to study the evolution of isolated vortices is the reduced-gravity model (one active layer over an infinite one) (Nof 1981, 1983a; Smith and Reid 1982; Davey and Killworth 1984).

In this paper, we seek to investigate the validity of the latter approximation and concentrate our attention on the following question: How deep does the lower layer of a two-layer system have to be to have a negligible influence on the dynamics of upper layer rings? To our knowledge, this question has not yet been answered, except in the very particular case of quasi-geostrophic dynamics (weak interface displacements) and uniform potential vorticity in the lower layer (Polvani et al. 1989). Yet, the answer to this question is important, for it would shed light on the applicability of the reduced-gravity model to the study of various oceanic phenomena dominated by geostrophic dynamics such as eddies, jet meanders and other mesoscale features.

Idealized isolated vortices overlying an infinitely deep lower layer on a β-plane translate toward the west due to the β-induced drift (e.g., Flierl 1977; Nof 1981, 1983a; Cushman-Roisin et al. 1990). However, a finite lower layer may significantly alter the rings' migration by introducing a form drag which, as frictional drag, opposes the drift (Flierl 1984). Furthermore, they may be vulnerable to baroclinic instability. Consequently, it is expected that in the actual ocean the lower-layer depth will play a rather important role in the ring's behavior. Specifically, it is expected that the form drag will slow down the westward migration rate and will introduce a significant meridional drift, or that the ring will become unstable.

In order to study the transition regime between a finite-depth system and the reduced-gravity approximation (infinitely deep second layer), a series of experiments are performed with a primitive-equation, isopycnic-coordinate two-layer numerical model whose upper-to-lower layer depth ratio is varied from 1/5 to 1/1000. By varying the depth over such a wide range, we shall be able to discern a lower-layer depth beyond which the reduced-gravity approximation is valid. The choice of the primitive equations has already been justified.

The advantages of the isopycnic coordinate system used here are first, that vertical resolution is concentrated in regions of strong horizontal density gradients such as fronts and second, lateral diffusion is along isopycnal surfaces, which are in general the preferred mixing surfaces of the ocean (Iselin 1939; Montgomery 1940). The model is therefore free of any artificial deterioration due to cross-isopycnal numerical diffusion. Finally, in this type of model, the specification of desired initial conditions through the positioning of the isopycnal surfaces is allowed and, in particular, the initial conditions of lenslike eddies; i.e. eddies where isopycnals surface, can be reproduced. The model used in this study was originally developed by Bleck and Boudra (1986).

The layout of the paper is as follows. In section 2, the model characteristics are reviewed, and a series of experiments with varying depth ratio for lenses, cyclones and anticyclones is presented. Section 3 then performs a scaling analysis of the two-layer system and determines the conditions needed for the lower layer to have a negligible influence on the dynamics of the upper layer. In section 4, a comparison between the numerical findings and the theoretical criterion is presented. Finally, the results are summarized in the concluding section.

2. Impact of a finite layer on the ring's behavior: Numerical results

In this section, the ring's behavior in a two-layer system is investigated by using the isopycnic coordinate numerical model of Bleck and Boudra (1986) configured in a two-layer, square domain on a β-plane. The eddy evolution is studied in detail as the layer depth ratio $\delta = H_1/H$ is varied from 1/5 (realistic oceanic ratio) to 1/1000 ("infinitely" deep lower layer), where H_1 is the mean upper layer thickness and H, the total depth. The model characteristics are first described in section 2a. In section 2b, analytical expressions for the westward drift of isolated eddies over an infinitely deep lower layer are briefly reviewed for comparisons with the numerical experiments of section 2c where the impact of the variation of the ratio δ on the ring's behavior is studied in detail. The initial conditions are kept identical for all experiments, except for the varying lower-layer thickness. Finally, section 2d investigates the effect on the results of section 2c of the lateral eddy viscosity A_M used in the numerical model.

a. The numerical model

The primitive equation, pure-isopycnic model of Bleck and Boudra (1986) may be viewed as a stack of shallow water models, each consisting of a momentum and a continuity equation:

$$\frac{\partial \mathbf{v}}{\partial t} + \mathbf{v}\cdot\nabla_\rho\mathbf{v} + \xi\mathbf{k}\times\mathbf{v} = -\nabla_\rho M + \alpha\frac{\partial \tau}{\partial z} + A_M h^{-1}\nabla_\rho\cdot h\nabla_\rho\mathbf{v}, \quad (1)$$

$$\frac{\partial h}{\partial t} + \nabla_\rho\cdot(h\mathbf{v}) = 0, \quad (2)$$

where $\xi = \zeta + f$ is the absolute vorticity ($\zeta = v_x - u_y$); $M = gz + p\alpha$ is the Montgomery potential; h is the thickness of a layer of constant density; the specific volume $\alpha = \rho^{-1}$; τ is the wind stress and A_M is the lateral viscosity. The subscript ρ indicates derivatives on surfaces of constant density. The layers commu-

nicate vertically through hydrostatically transmitted pressure forces. For more detail on the numerical model, the reader is referred to Bleck and Boudra (1986).

The model is configured in a two-layer 2000 km $\times$ 2000 km square domain on a β-plane with a grid spacing of either 20 or 10 km. Lateral boundary conditions are free-slip everywhere. A rigid lid and a flat bottom are chosen as upper and lower boundaries. The model is initialized with a Gaussian distribution of the upper layer thickness, $h = H_1 + h_o e^{-r^2/2L^2}$ where r is the radius from the center, L, the radius of maximum velocity and h_o, the interface displacement at the eddy center. This is not necessarily the most realistic parameterization of an oceanic eddy (Olson 1980), but it does permit comparison with other studies (McWilliams and Flierl 1979; Mied and Lindeman 1979; Smith and Reid, 1982; McWilliams et al. 1986). The velocities are initially in geostrophic balance in the upper layer and at rest below. This implies that, shortly after initialization, there will be a readjustment of the flow toward a gradient wind balance on the β-plane. This slight imbalance in the initial conditions does not affect the long-term evolution of the ring. The baroclinic motion of the two layers is coupled by the motion of the interface, which produces vortex-tube compression in one layer and stretching in the other (Pedlosky 1987). The reduced gravity g' is fixed and equal to 0.0196 m s^{-2}. The values for f_o and β_o are 9.3×10^{-5} s^{-1} and 2×10^{-11} m^{-1} s^{-1}, respectively. All numerical simulations are 200 days long. The values for L and h_o are chosen to be 60 km and 500 m, respectively. The lateral eddy viscosity A_M is maintained constant at 330 m^2 s^{-1}, except in section 2d. In the rest of the paper, cyclones and anticyclones are defined as eddies whose undisturbed depth does not vanish along their rim while lenses are defined as anticyclonic eddies whose isopycnals surface.

b. *The westward drift of eddies over an infinitely deep lower layer*

Several expressions for the westward drift of eddies over an infinitely deep lower layer have been derived by different authors and they are briefly reviewed here for comparisons with the numerical experiments of the following section. The case of anticyclonic lenses was first studied by Nof (1981) and Killworth (1983). It was found that the essence of the drift is due to the balance of an equatorward β-induced force by the poleward Coriolis force associated with the drift. Cyclones and anticyclones were first discussed analytically by Flierl (1977) and Nof (1983a). The latter showed that, in addition to the two forces mentioned above, a third force results from the upper-layer fluid circulating around the eddy. Recently, using a scaling analysis similar to that presented later in section 3, but for a single layer, reduced-gravity model, Cushman-Roisin et al. (1990) derived another expression for the westward propagation. The latter becomes identical to Nof's formula when the geostrophic approximation is made and is obtained with fewer restrictions, namely the eddy does not have to keep a constant shape and to move westward at a constant speed. On the other hand, the centrifugal force was not retained. There is therefore a trade-off between the different theories. For more details, the reader is referred to Nof (1983a) and Cushman-Roisin et al. (1990).

Using the Cushman-Roisin et al. (1990) formula, the westward drift can be simply expressed as $\beta_o \tilde{R}_d^2$ with $\tilde{R}_d^2$ defined as $g'\tilde{H}/f_o^2$ and $\tilde{H} = H_1 + \frac{1}{2} \times \iint \eta^2 / \iint \eta$, where η is the variation of the upper layer thickness defined as $h = H_1 + \eta$. Hence, it is possible to state that an isolated eddy will translate at the speed of a long Rossby wave defined from the undisturbed depth corrected by half the average interfacial displacement over the eddy. Cyclones will therefore move slower ($\eta < 0$) than the long Rossby wave speed $\beta_o R_d^2$ (calculated from the undisturbed depth) while anticyclones ($\eta > 0$) will move faster, a result first pointed out by Nof (1983a). In the particular case of lenses ($H_1 = 0$), an outside long Rossby wave speed cannot be defined and the lens will then travel at the speed $\beta_o \tilde{R}_d^2$ with $\tilde{H} = \frac{1}{2} \iint \eta^2 / \iint \eta$.

c. *Variation of the layer depth ratio: Numerical experiments*

1) LENSES

In this case, the upper-layer thickness H_1 is set equal to zero. The westward propagation speed of the lens center (defined as the maximum interface displacement) does not vary as the ratio δ (defined as h_o/H_2) changes. In all experiments, the lens is observed to move slowly westward with no appreciable meridional motion, except perhaps during an initial adjustment period. If δ is greater than 1/50, the lens becomes unstable. At the ratio 1/25, a perturbation with wavenumber 2 develops on the edge of the lens while with a ratio 1/10, the lens breaks into two pieces. Therefore, as δ increases, the coupling between the two layers intensifies and generates baroclinic instabilities. For this set of parameters, the ratio 1/50 appears to be small enough for the lower layer to have a negligible impact on the lens dynamics. For a review on the stability of ocean vortices, the reader is referred to Ripa (1989).

Expressions for the westward drift speed of a lens (see section 2b) were derived for the center of mass of the eddy (C_M), which is traditionally though to be a good representation of the eddy center. How good is this approximation since the eddy center is generally defined as being the extremum of either the interface displacement (η) or potential vorticity (q) distribution? In order to compare the propagation rates of these three centers (C_M, C_η and C_q) in the lens case, their locations

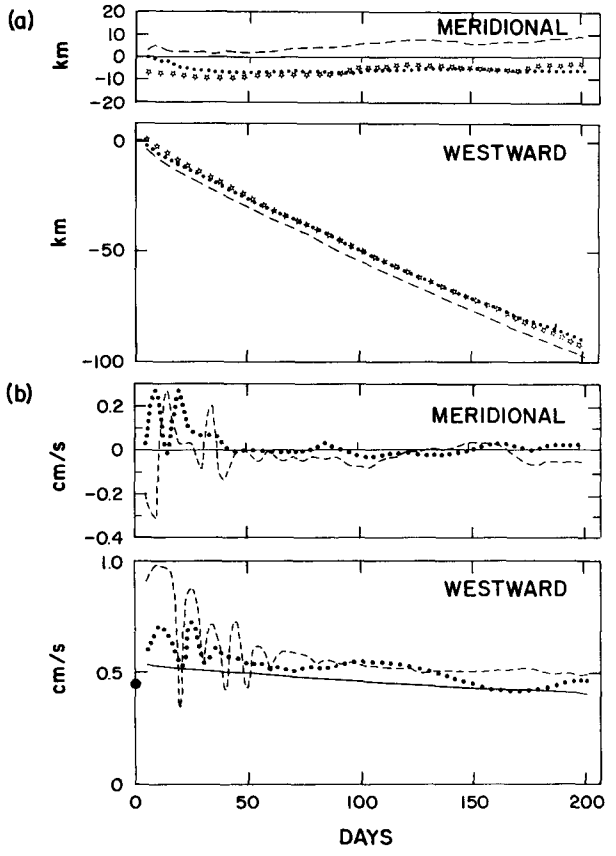

FIG. 1. Lens with $\delta = 1/1000$. Westward and meridional displacement (a) and propagation speeds (b) of the center of mass C_M (dotted), interface displacement extremum C_η (dashed) and potential vorticity extremum C_q (stars). Also represented are estimates of the center of mass westward drift from Nof (1981) (solid dot) (using an equivalent linear velocity profile) and Cushman-Roisin et al. (1990) (solid line) (computed from the eddy structure).

versus time for the ratio 1/1000 are presented in Fig. 1a. The center of mass is located behind the eddy center, defined from the interface displacement; C_q is observed to follow closely the center of mass. There is no significant meridional motion for either of them, except a slight poleward motion of C_η. The zonal and meridional velocities of the center of mass and eddy center versus time are presented in Fig. 1b and are compared to estimates of the center of mass westward drift (Nof 1981; Cushman-Roisin et al. 1990). The estimates represent accurately the westward drift of the numerical simulations (center of mass or eddy center since both move at approximately the same speed in this lens case). That is to say, when the lower layer has negligible effect (ratio δ between 1/1000 and 1/50), the numerical results are in agreement with the analytical predictions.

In the lens case, only the form drag of the lower layer can induce a meridional drift because interactions with an upper-layer wake are excluded by virtue of the outcropping interface (Flierl 1984). Like a frictional drag, the form drag is directed in the opposite sense to the migration, and there is no force to balance it until the direction of migration is altered in such a manner that a component of the β-induced force can oppose it (Nof 1983b; Flierl 1984). This can be achieved in the lens case only by the introduction of an equatorward drift. No appreciable meridional displacement is observed in our numerical simulations. This result does not agree with the analytical work of Flierl (1984) which predicts a meridional velocity of 0.15 cm s^{-1} for the Gaussian eddy and $\delta = 1/50$. This is not surprising since the Flierl (1984) theory requires $\Delta = h_o f_o / H\beta_o L \ll 1$, a criterion not verified by the above numerical experiment ($\Delta = 5$).

2) ANTICYLCLONES AND CYCLONES

The upper layer thickness H_1 is now set equal to 1000 m, and the perturbation thickness h_o is chosen either positive or negative. The propagation speeds for both anticyclones and cyclones are presented in Fig. 2 as δ varies. As δ decreases, the westward translation speed increases while the meridional drift decreases. Both reach an asymptotic value for $\delta < 1/50$. A similar result is obtained for the trajectories (Fig. 3) and for the kinetic and available potential energies versus time (Fig. 4). Anticyclones are observed to move faster than the cyclones as discussed in section 2b.

To illustrate the difference of behavior in the presence of an "infinite" lower layer, the time evolution of two anticyclones (A1 and A2) and cyclones (C1 and C2) with $\delta = 1/5$ and $\delta = 1/1000$, respectively, are presented in Figs. 5a,b and 6a,b. They are consistent with the previous results of McWilliams and Flierl

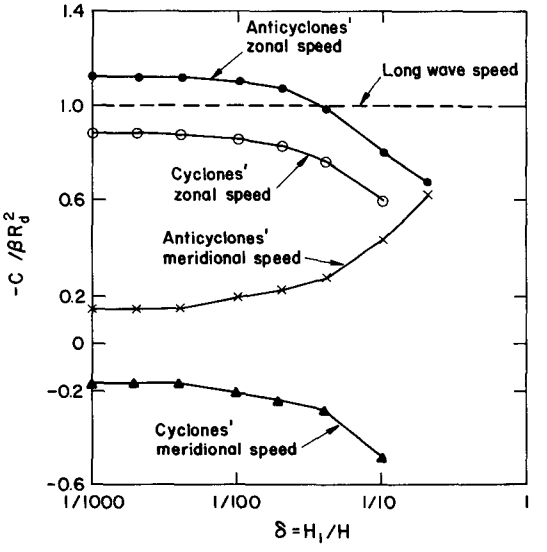

FIG. 2. Propagation speeds of both anticyclones and cyclones as a function of the ratio $\delta = H_1/H$. The Rossby radius of deformation is defined by $R_d = \sqrt{g'H_1}/f_o$. Adapted from Chassignet and Nof (1989).

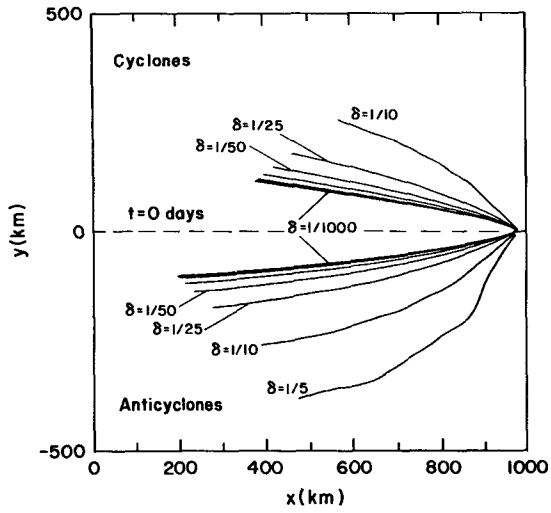

FIG. 3. Trajectories of the center (defined from the interface displacement) for both anticyclones and cyclones as a function of the ratios $\delta = H_1/H$ of Fig. 2.

(1979), Mied and Lindemann (1979), Smith and Reid (1982), Matsuura and Yamagata (1982), Davey and Killworth (1984) and McWilliams et al. (1986). The major differences between A1 and A2, on one hand, and C1 and C2, on the other, are, as mentioned earlier, a more rapid westward propagation speed and a smaller meridional displacement. As the thickness of the lower layer increases, the meridional displacement of the ring decreases due to a smaller form drag of the lower layer on the upper-layer eddy. In A2 and C2, the only factor remaining important for the meridional displacement is the interaction with the Rossby wave wake. If this effect is suppressed, the ring should move purely westward, which is precisely the case with a lens over an "infinite" lower layer as shown previously. A major difference between cyclones and anticyclones is that in the experiment with the larger δ value, the cyclones have the tendency to succumb to baroclinic instability, and to break in several pieces. This is the case for C1 ($\delta = 1/5$) around day 100 as confirmed by a sustained rise in lower layer kinetic energy (Fig. 4b) and a rapid decrease in available potential energy (Fig. 4d). As the ratio δ decreases, the cyclones are more stable because the coupling between the two layers becomes weaker and baroclinic instability less effective. On the contrary, anticyclones appear to be stable for all values of δ. A discussion on why anticyclonic eddies are, in general, more robust than their cyclonic counterparts can be found in Cushman-Roisin and Tang (1990).

In comparing the locations and propagation speeds of the three centers (C_M, C_η and C_q) for one simulation with the ratio 1/1000 (anticyclone A2), the center of mass is always found to be located ahead of the eddy center, be it defined from the interface displacement or potential vorticity. It also reveals almost no meridional displacement, while the eddy center (defined from either C_η or C_q) exhibits a significant equatorward displacement (Fig. 7a). The meridional drift of the center of mass is almost zero, while the meridional drift of the eddy center is significant. The meridional drift of the center of mass therefore does not mimic accurately that of the eddy center. In summary, the theoretical propagation speed of the center of mass (see section 2b) is quite a good approximation for the westward component of the drift, but is not for its meridional component. The propagation of the energy centers (weighted by either potential or kinetic energy) is discussed by Smith and Reid (1982). As in the lens case, Nof (1983a) and Cushman-Roisin et al. (1990) estimates of the westward drift for an infinitely deep lower layer are in agreement with the numerical simulations when the lower layer has negligible effect (ratio δ between 1/1000 and 1/100) (Fig. 7b).

Energy considerations can further illustrate the meridional drift of isolated eddies. Since the Rossby-wave radiation in the upper and lower layer and associated form drag cause the eddies to loose energy, they tend to approach their so-called "latitude of rest" (Larichev 1983) where, due to changes in the planetary vorticity, their relative vorticity and, hence, kinetic energy vanish. If the center of the vortex is defined as the extremum of potential vorticity, then the particle located at the center should remain at the center in order to conserve its potential vorticity. Expressing the potential vorticity q of the particle at the center as

$$q_{\text{center}} = \frac{f_o + \beta_o y_{\text{center}} + \zeta_{\text{center}}}{h_{\text{center}}} \tag{3}$$

where ζ is the vorticity of the particle, with q_{center} constant, we can state that, at a certain time Δt later, the change in y_{center} is given by

$$\Delta y_{\text{center}} = \frac{q_{\text{center}}}{\beta_o} \Delta h_{\text{center}} - \frac{1}{\beta_o} \Delta \zeta_{\text{center}}. \tag{4}$$

This simple definition of Δy_{center} illustrates the poleward and equatorward drift of the cyclones and anticyclones, respectively. Indeed, radiation of energy implies a decrease in both the interface displacement and the magnitude of the vorticity within the eddy. In the Northern Hemisphere, for an anticyclone Δh is negative and $\Delta \zeta$ positive (since ζ is negative), which therefore implies from (4) a southward motion. On the contrary, for a cyclone, Δh will be positive and $\Delta \zeta$ negative, therefore implying a northward motion. Other mechanisms also induce meridional motion (Chassignet 1989).

Cyclone C1 is a close approximation, except for the value of the lateral viscosity, to the eddy in experiment 10 of Mied and Lindemann (1979). They did not find any persistent structure for any length of time in the lower layer. Their interpretation was that, in the limit of $H_1/H_2 \ll 1$, the lower ocean is decoupled from the upper ocean. As shown above, when $\delta < 1/50$, the

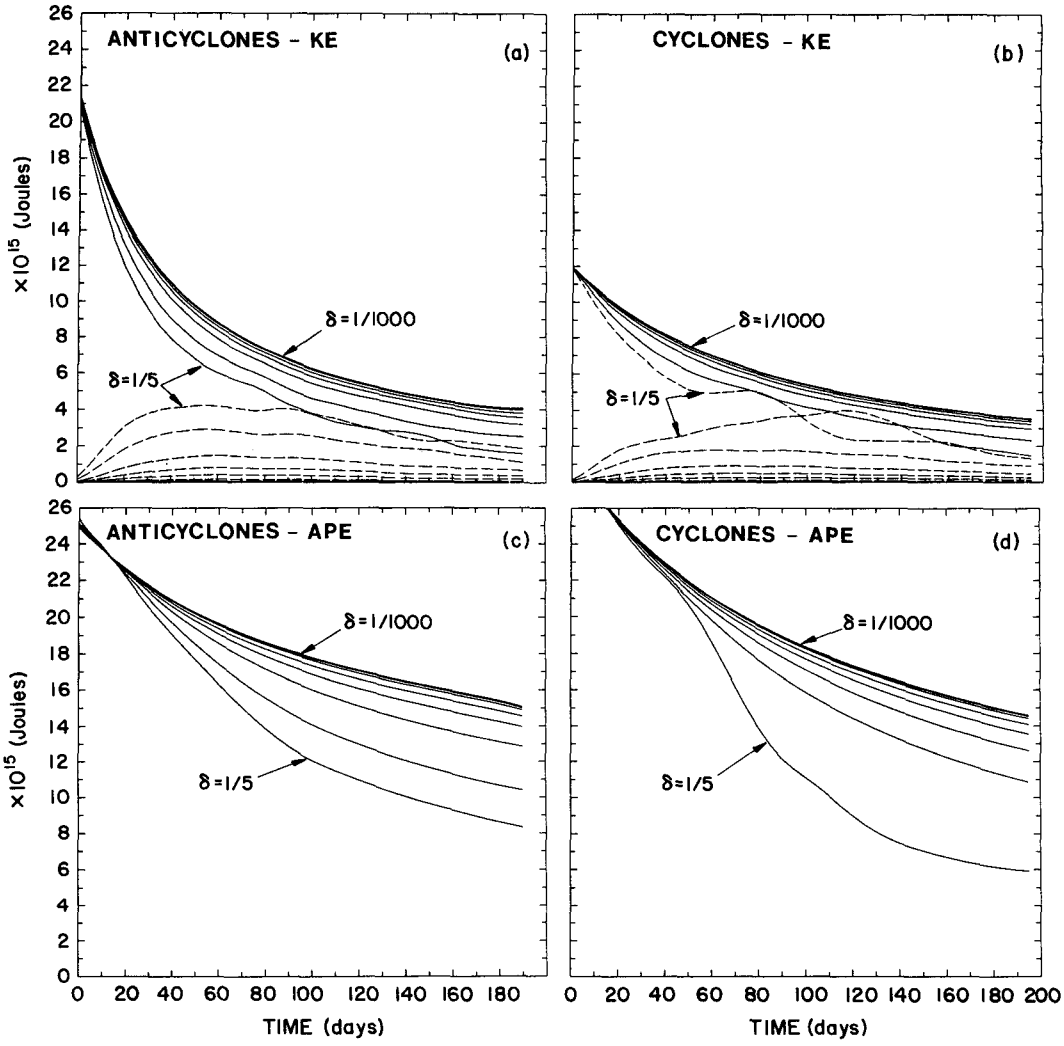

FIG. 4. Kinetic and available potential energy for anticyclones and cyclones for the various thickness ratio δ of Fig. 2. (a) and (b) Kinetic energy versus time. The upper and lower curves correspond to the upper and lower layer, respectively. (c) and (d) Available potential energy versus time.

influence of the lower layer on the upper layer vortex seems to become negligible, but it can be seen in Figs. 5b and 6b that a compensating flow is always present in the lower layer. This counter circulation is located in the lower layer behind the upper layer ring. McWilliams et al. (1986) found a similar result and attributed this circulation as part of the radiation field.

d. *Variation of the lateral eddy viscosity A_M*

In the previous section, the behavior of lenses, cyclones and anticyclones was discussed as the ratio δ was varied. In the above experiments, the viscosity was fixed to 330 $m^2 s^{-1}$. This value was chosen initially to permit comparisons with general circulation models results (Chassignet et al. 1990), where high viscosity is required for numerical stability. In order to illustrate the impact of A_M on the ring's behavior, the trajectories of A1 ($\delta = 1/5$) and A2 ($\delta = 1/1000$) are displayed in Fig. 8 as A_M is varied from 330 to 0 $m^2 s^{-1}$. When the ratio $\delta = 1/5$, varying A_M induces substantial changes in the anticyclone's propagation (Fig. 8). On the contrary, when $\delta = 1/1000$, the changes are small. In the latter case, the coupling between the two layers is very weak and dissipation occurs mostly in the upper layer. For a discussion on the nonfrictional decay of mesoscale eddies in a reduced-gravity model, the reader is referred to Smith and Reid (1982). With $\delta = 1/5$, dissipation occurs in both layers. With low values of the lateral eddy viscosity A_M (small dissipation), a strong circulation is present in the lower layer which, because of the significant coupling between the two layers, modifies significantly the anticyclone behavior. The results obtained in the previous section are there-

fore somewhat dependent on the choice of the lateral eddy viscosity A_M, at least for high δ. On the other hand, in the cases with very low values of A_M, energy is found to accumulate in the small scales as shown in Fig. 9, even if the model is numerically stable. In the numerical model used in this study, the latter process becomes negligible for A_M greater than 50 $m^2\ s^{-1}$. In the context of a general circulation model with forcing, such an accumulation of energy in the small scales will lead to numerical instability if A_M is smaller than 100 $m^2\ s^{-1}$ (Chassignet et al. 1990).

3. Scaling analysis

In order to illustrate the results of the previous section, we now perform in this section a scaling analysis of the two-layer system with emphasis on the geostrophic regimes which dominate oceanic features such as rings (McWilliams 1991). Estimates of the Rossby number (ϵ), compiled from 30 observed oceanic rings (Chassignet et al. 1990), vary between 0.1 and 0.2 for warm-core rings and 0.1 and 0.4 for cold-core rings and, at a first approximation, it is therefore reasonable to consider that most eddies have a small Rossby number. Mesoscale eddies in the ocean can be categorized as being either quasi-geostrophic in the open ocean ($L \sim R_d$, $h_o \ll H_1$; Kamenkovich et al. 1986) or frontal-geostrophic in the vicinity of western boundary currents ($L > 3R_d$, $h_o \sim H_1$; Olson et al. 1985; Chassignet et al. 1990) where H_1 is the upper layer thickness; h_o, the interface displacement at the center of the eddy; L, the eddy length scale and $R_d = (g'H_1)^{1/2}/f_o$, the internal Rossby radius of deformation. Within certain restrictions, the dynamics in the single layer of a reduced-gravity system are dominated by a geostrophic balance (Williams and Yamagata 1984; Cushman-Roisin 1986; Cushman-Roisin and Tang 1990) and inertial–gravity waves can be filtered out yielding a generalized geostrophic equation. One can anticipate that, under similar conditions, a two-layer system would also possess a variety of geostrophic regimes. Naturally, motions in a second layer allow for the presence of baroclinic instability, an important process excluded from the simpler, reduced-gravity system. One expects that, as the lower-layer thickness of a two-layer system is increased, the dynamics should revert to those of the one active layer.

We make the following assumptions: flat bottom, β-plane, rigid lid and a lower layer at least as deep as the upper layer. The last assumption is in keeping with actual oceanic stratification. Although it does eliminate certain dynamical regimes, namely those involving a shallow bottom layer under a deeper upper layer, the latter regimes are mirrored by analogs with the vertically reverse layering configuration. The notation is as follows: $H_1 + \eta$ is the upper layer thickness and, H, the total depth. The subscripts 1 and 2 refer to the upper and lower layers, respectively with ρ_i, density, u_i and v_i, eastward and northward velocity components, p_i, dynamical pressure and h_i, layer thickness.

With the Coriolis parameter noted as $f = f_o + \beta_o y$, the equations of motion, with understood subscripts, are

$$u_t + uu_x + vu_y - fv = -p_x \tag{5}$$

$$v_t + uv_x + vv_y + fu = -p_y \tag{6}$$

$$h_t + uh_x + vh_y + h(u_x + v_y) = 0 \tag{7}$$

where, for each layer, the dynamical pressure and thickness are obtained from

$$p_1 = \pi + g'\eta, \quad p_2 = \pi \tag{8}$$

$$h_1 = H_1 + \eta, \quad h_2 = H - H_1 - \eta. \tag{9}$$

Here, π is the lower-layer pressure and g' is the reduced gravity [$g' = g(\rho_2 - \rho_1)/\rho_2$]. With the present notation, the choice of variables for the barotropic and baroclinic modes are the lower-layer dynamical pressure, π, and the interface displacement, η, respectively. The influence of the lower layer will be deemed negligible when and only when the terms involving π in the equation governing the evolution of η are small and negligible.

With initial conditions characterized by an interface deformation field of length scale L (not necessarily R_d) and amplitude h_o (not necessarily H_1), the variables can be scaled as follows:

x and y by L, η by h_o, p_1 by $g'h_o$ (from (8)),

u_1 and v_1 by U_1

$= g'h_o/f_oL$ (geostrophy), p_2 and π by P,

u_2 and v_2 by U_2

$= P/f_oL$ (geostrophy) and time by T.

The scales for the barotropic pressure field, P, and the time, T, are considered to be determined by the dynamics. The reasoning is as follows: following an initial baroclinic perturbation (interface displacement), the system will evolve at its own time scale and will generate barotropic motions of its own choosing.[1] Next, a series of dimensionless numbers are defined

- *External parameters:* fixed by geometry
  Depth ratio: $\delta = H_1/H$
- *Primary parameters:* related to amplitude and length scales of flow field
  Rossby number: $\epsilon = U_1/f_oL = g'h_o/f_o^2L^2$
  Burger number: $s = g'H_1/f_o^2L^2$

[1] One could imagine initial and/or boundary conditions including a barotropic flow of strength other than otherwise developed by the system, and cases of time-varying boundary forcing introducing an external time scale. But, in order to emphasize the properties of the two-layer system, such independent scales are excluded from the present formalism.

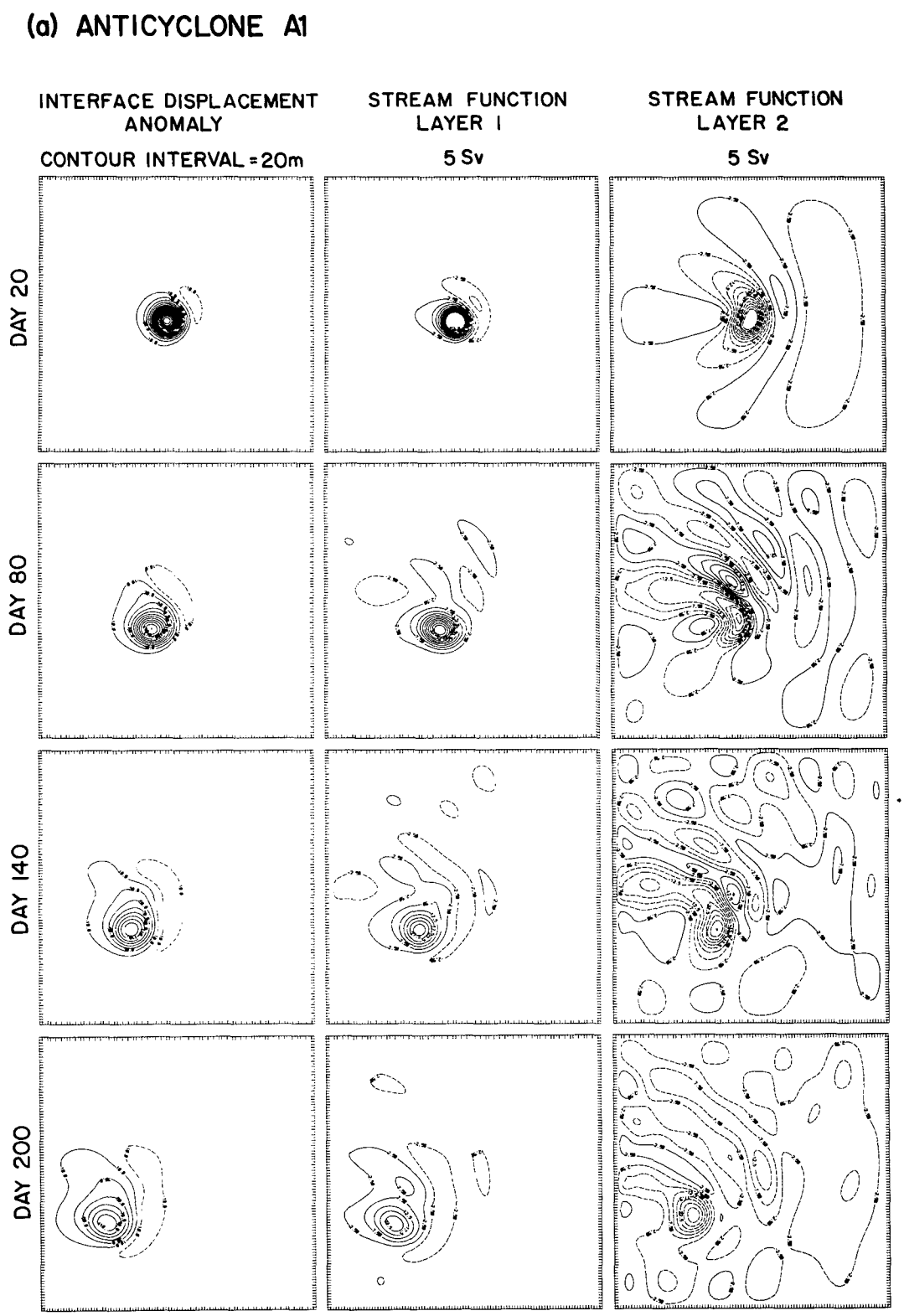

FIG. 5. Evolution of interface displacement and streamfunction in each layer for (a) anticyclone A1, h_o = 500 m, H_1 = 1000 m, H_2 = 4000 m (shallow lower layer) and for

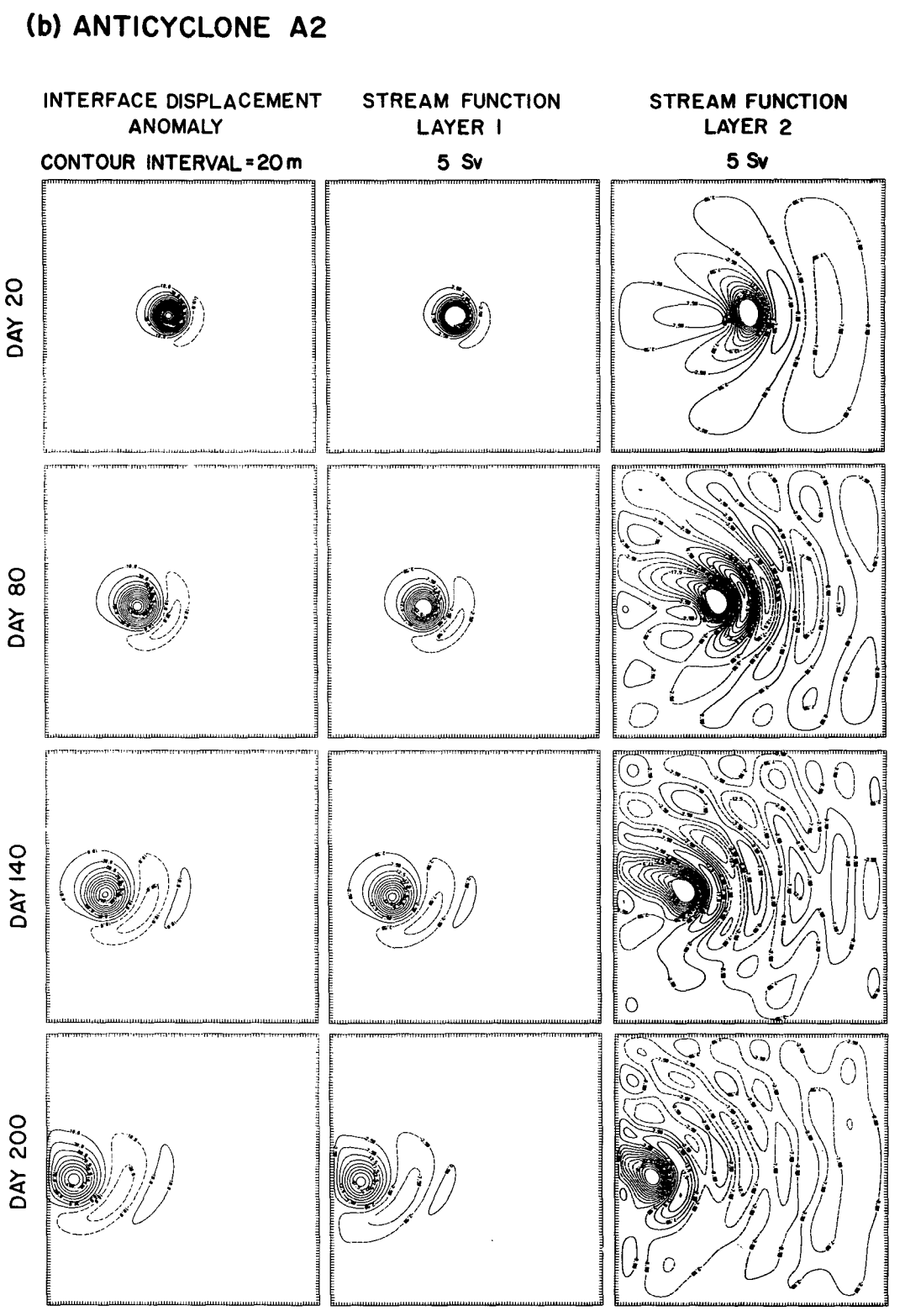

FIG. 5. (*Continued*) (b) anticyclone A2, h_o = 500 m, H_1 = 1000 m, H_2 = 999 000 m (deep lower layer). The streamfunctions are computed from the rotational part of the mass transport after decomposition into its rotational and divergent components.

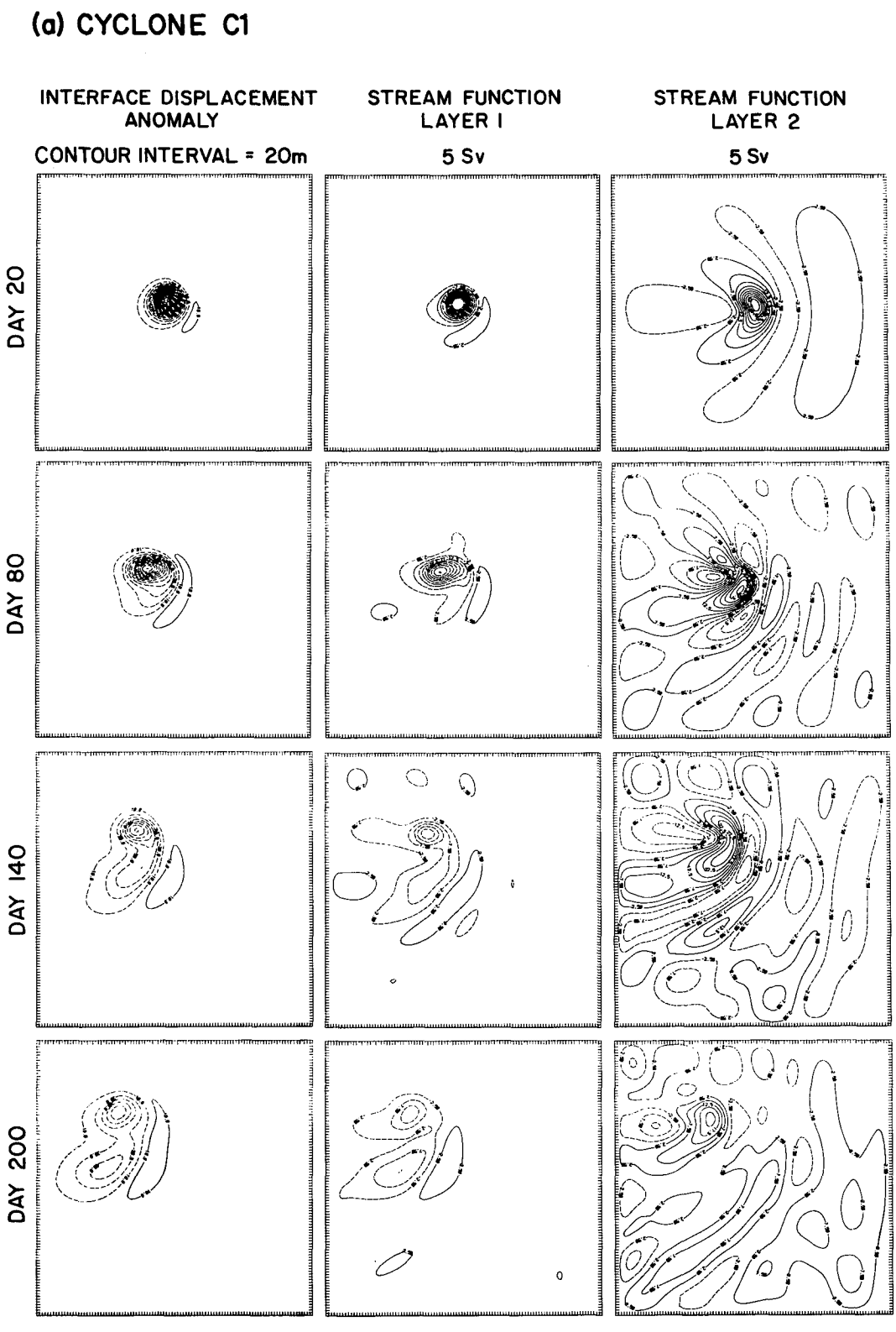

FIG. 6. As in Fig. 5 for (a) cyclone C1, h_o = 500 m, H_1 = 1000 m, H_2 = 4000 m (shallow lower layer) and for

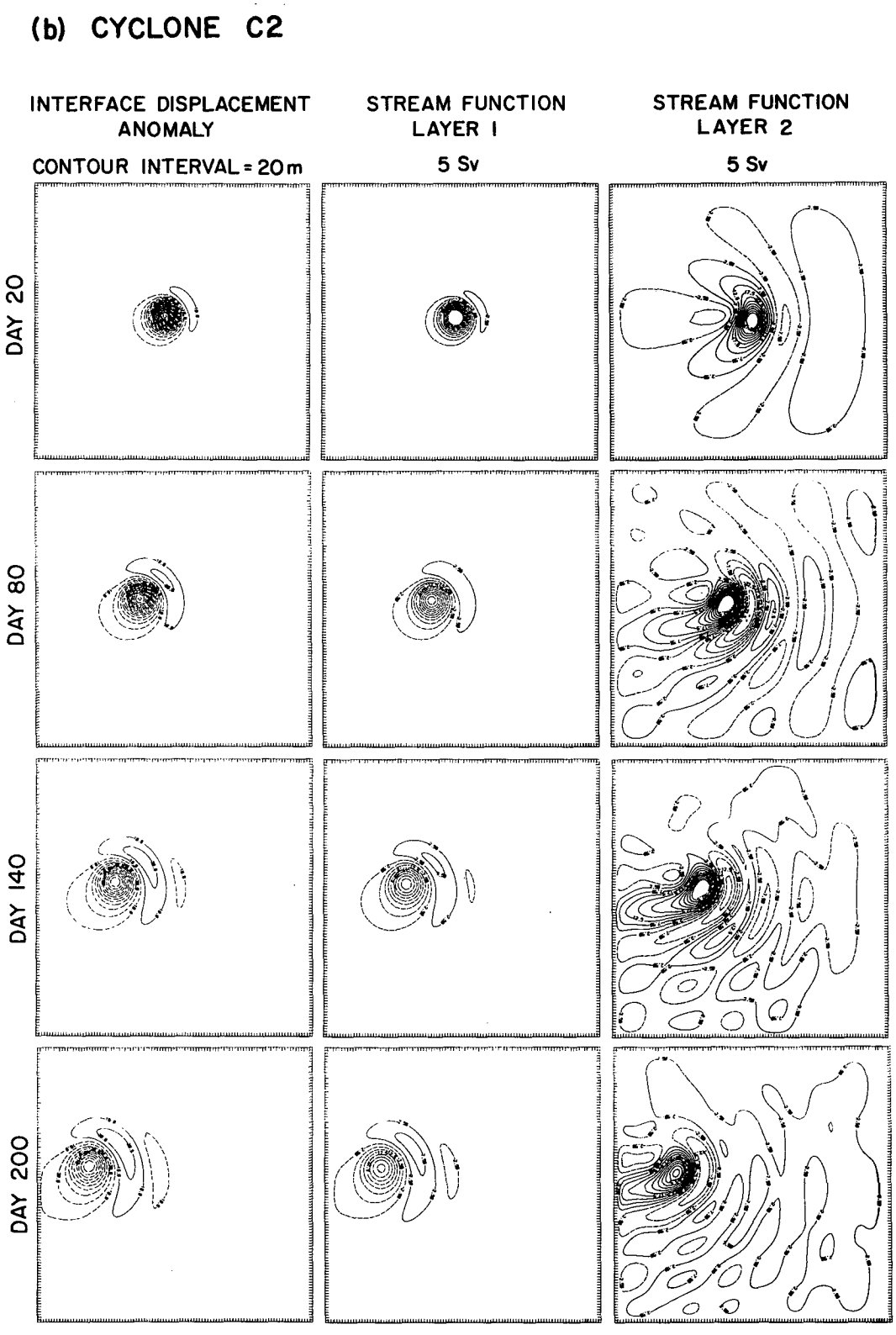

FIG. 6. (*Continued*) (b) cyclone C2, h_o = 500 m, H_1 = 1000 m, H_2 = 999 000 m (deep lower layer).

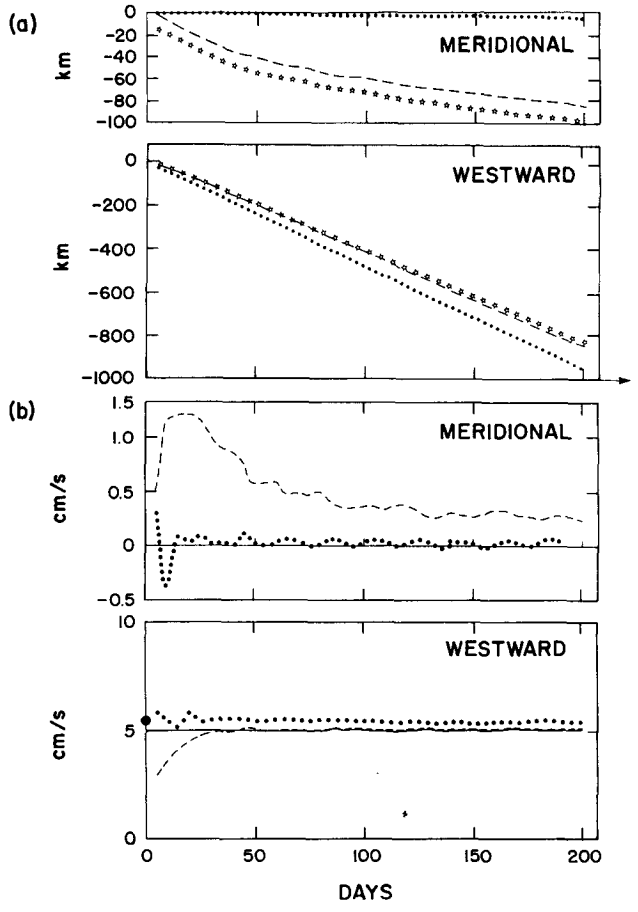

FIG. 7. Anticyclone A2. Westward and meridional displacement (a) and propagation speeds (b) of the center of mass C_M (dotted), interface displacement extremum C_η (dashed) and potential vorticity extremum C_q (stars). Also represented are estimates of the center of mass westward drift from Nof (1981) (solid dot) (using an equivalent linear velocity profile) and Cushman-Roisin et al. (1990) (solid line) (computed from the eddy structure).

Beta number: $\beta = \beta_o L/f_o$

- *Secondary parameters:* related to barotropic flow field and time scale

  Pressure ratio: $\gamma = P/g'h_o$

  Dimensionless frequency: $\omega = 1/f_o T$

These numbers are subject to several inequalities. First, by definition, δ must be less than unity, but, moreover, since the lower layer is at least as deep as the upper layer, it follows that $\delta \leqslant 1/2$, $1/2 \leqslant 1 - \delta < 1$ and thus $1 - \delta$ will always be on the order of unity. If h_o were to exceed H_1, H_1 could be redefined as h_o; hence $h_o \leqslant H_1$ and $\epsilon \leqslant s$. The validity of the β-plane approximation requires that the changes in f to be much less than f_o, i.e. $\beta \ll 1$, while the choice of seeking geostrophic regimes demands $\epsilon \ll 1$ and $\omega \ll 1$. Finally, since the barotropic pressure field is viewed here as a reaction to an existing baroclinic flow field, one anticipates that P will be less than or at the most of the order of $g'h_o$, i.e. $\gamma \leqslant 1$. To recapitulate, the inequalities are

$$\delta < 1, \quad 1 - \delta = O(1), \quad \epsilon \leqslant s, \quad \gamma \leqslant 1,$$
$$\beta \ll 1, \quad \epsilon \ll 1, \quad \omega \ll 1. \tag{10}$$

Since the time scale and amplitude of the barotropic pressure field are to be determined by the dynamics, their respective inequalities ($\omega \ll 1$ and $\gamma \leqslant 1$) will have to be verified a posteriori.

The scaling analysis of Eqns. (5–9) is presented in appendix A and yields the following expressions of ω and γ. For all length scales,

$$\omega = \frac{\max(\gamma\epsilon,\ s\epsilon,\ s\beta)}{\max(s,\ 1)}. \tag{11}$$

For length scales shorter than or equal to the deformation radius ($s \geqslant 1$)

$$\gamma = \delta \tag{12}$$

while for longer length scales ($s < 1$),

$$\gamma = \delta \frac{\max(\epsilon,\ \beta)}{\max(s\epsilon,\ \gamma\epsilon,\ \beta)}. \tag{13}$$

At this point, a number of possible inequalities must be investigated one by one, and this task is not repeated here. The complete solution is presented graphically in Fig. 10, and the reader may verify that this is indeed the solution of the problem. One notes that the values of ω and γ are bounded by $\omega \leqslant \max(\epsilon, \beta)$ and $\delta \leqslant \gamma \leqslant \delta^{1/2}$. Since $\epsilon \ll 1$, $\beta \ll 1$ and $\delta < 1$, it is verified a posteriori that $\omega \ll 1$ and $\gamma \leqslant 1$.

With ω and γ determined, one is now in a position to discern the regimes for which the presence of motion

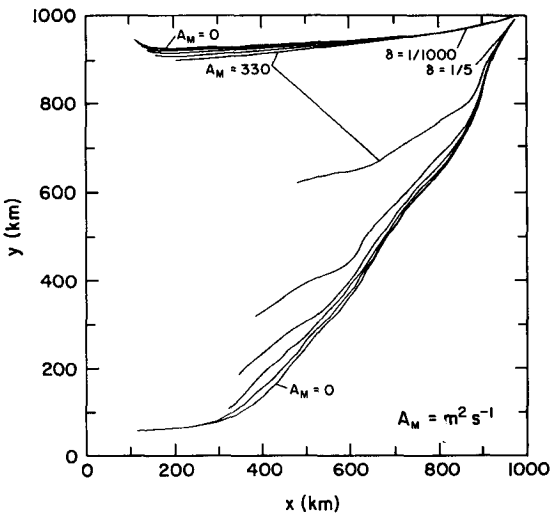

FIG. 8. Trajectories for anticyclones for varying lateral eddy viscosity, A_M, (330, 100, 50, 25, 10 and 0 m^2 s^{-1}) with depth ratio δ = 1/5 and 1/1000, respectively.

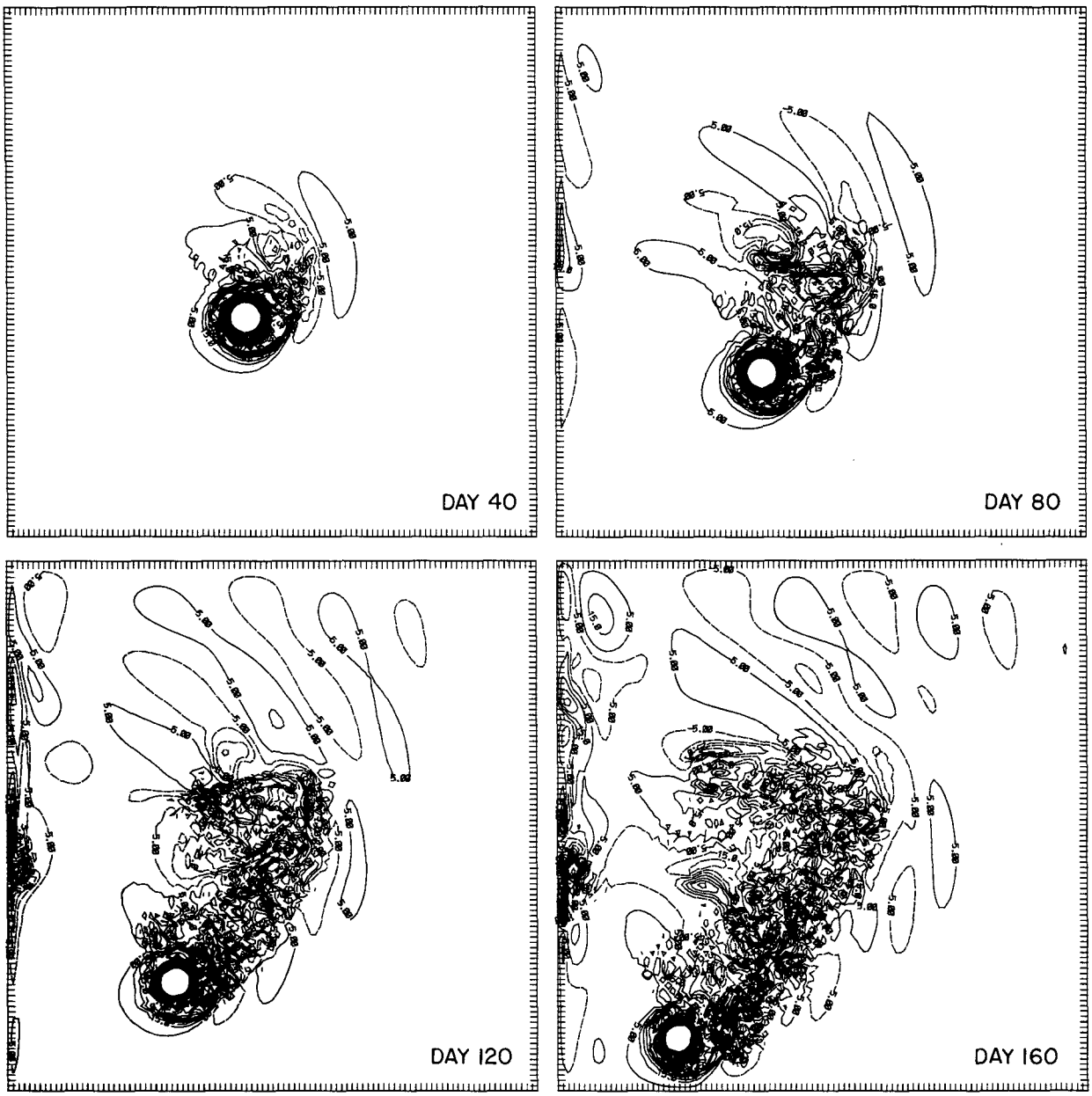

FIG. 9. Vorticity field of anticyclone A1 with lateral eddy viscosity $A_M = 5\ \mathrm{m^2\ s^{-1}}$.

in the lower layer does not affect the dynamics in the upper layer. The following equation (appendix A)

$$\omega \frac{\partial}{\partial t}(s\nabla^2\eta + s\gamma\nabla^2\pi - \eta) - \gamma\epsilon J(\pi, \eta) + s\epsilon J(\eta + \gamma\pi, \nabla^2\eta + \gamma\nabla^2\pi) + \epsilon^2 J(\eta, \eta\nabla^2\eta + \frac{1}{2}\nabla\eta\cdot\nabla\eta) + s\beta(\eta_x + \gamma\pi_x) + \beta\epsilon\eta\eta_x = 0. \quad (14)$$

results from the upper-layer momentum and continuity equations and, hence, governs the upper-layer dynamics. There will be no influence from the lower-layer flow field as long as all terms in π are negligible. As a result, the criterion specifying how deep the lower layer has to be to justify using the one-layer, reduced-gravity model is

$$\max(\omega s\gamma, \gamma\epsilon, s\gamma\epsilon, s\beta\gamma) \ll \max(s\omega, \omega, s\epsilon, s\beta). \quad (15)$$

Then, one notes that if $\delta = O(1)$ (i.e., both layers have about equal depths), $\gamma = O(1)$ (see Fig. 10), $s\omega \leq \omega\max(1, s) = \max(\epsilon, s\epsilon, s\beta)$, and the above inequality leads to

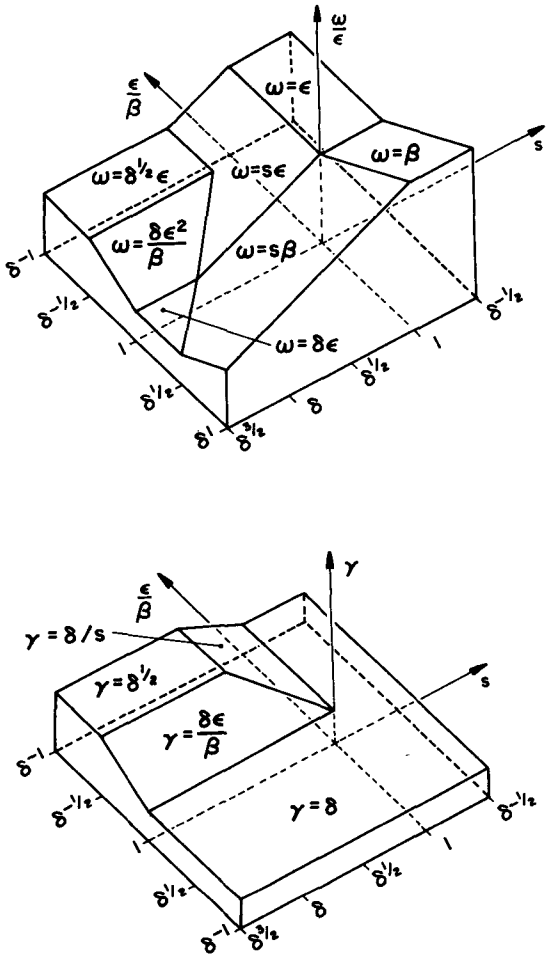

FIG. 10. Values of the secondary parameters ω and γ as functions of the primary parameters s, ϵ and β.

$$\max(\epsilon, s\epsilon, s\beta) \ll \max(\epsilon, s\epsilon, s\beta),$$

which obviously can never be met. Hence and not too surprisingly, a prerequisite is $\delta \ll 1$, namely a very deep lower layer. The question is now how deep.

For length scales shorter than or equal to the deformation radius ($s \geq 1$), $\omega = \max(\epsilon, \beta)$, $\gamma = \delta$ and inequality (15) becomes

$$\max(s\delta\epsilon, s\beta\delta) \ll \max(s\epsilon, s\beta),$$

and $\delta \ll 1$ is sufficient. For longer length scales ($s < 1$), inequality (15) is best solved graphically. In each region of Fig. 11, the corresponding values of ω and γ are substituted in (15), and hatched areas correspond to regions where inequality (15) is impossible.

Unhatched areas of Fig. 11 are regions where inequality (15) is met, and thus where the one-layer, reduced-gravity model applies. Examination of the results leads to the condition $\delta \ll s^2$ when $\epsilon/\beta \geq 1/s$ and $\delta \ll \min(1, s\beta/\epsilon)$ when $\epsilon/\beta \leq 1/s$.

One inequality that recapitulates all possible cases is

$$\delta \ll \min\left[1, \max\left(s^2, \frac{s\beta}{\epsilon}\right)\right], \tag{16}$$

which is the desired criterion formulated in terms of the dimensionless numbers of the problem. Returning to the original scales, this criterion becomes

$$H \gg \max\left[H_1, \min\left(H_1 \frac{L^4}{R_d{}^4}, h_o \frac{L_\beta}{L}\right)\right], \tag{17}$$

where R_d and L_β are the radius of deformation and planetary scale defined as $\sqrt{g'H_1}/f_o$ and f_o/β_o, respectively. On the f-plane, expression (17) reduces to

$$H \gg \max\left(H_1, H_1 \frac{L^4}{R_d{}^4}\right). \tag{18}$$

Hence, at horizontal scales up to the deformation radius, a lower layer much deeper than the upper layer is sufficient. For increasing length scales beyond the deformation radius, on both the f- and β-planes, the reduced-gravity model rapidly loses its validity. The model recovers its validity toward larger scales on the β-plane.

Because it is derived in the context of geostrophic dynamics (small Rossby number, ϵ), the question arises as to whether criterion (17) is applicable to ageostrophic motions when the length scale, L, is on the order of the deformation radius, R_d, and simultaneously, the amplitude scale, h_o, is on the order of the upper-layer depth, H_1. However, the case of fully ageostrophic motion is quite elementary, and its analysis is presented in appendix B. It is then shown that criterion (17), derived for geostrophic motions, also applies to ageostrophic motions.

In the limit of the reduced-gravity model, two processes are excluded, namely barotropic motion and baroclinic instability. The importance of the latter as the lower layer depth is varied and its analogy to cri-

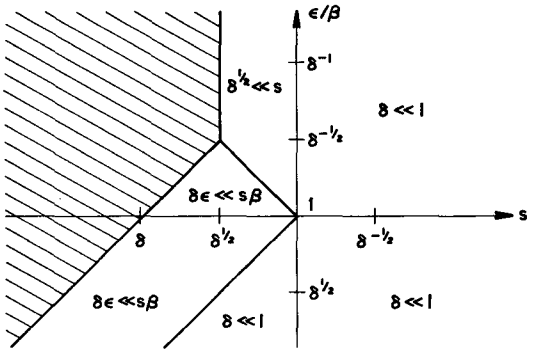

FIG. 11. Application of inequality (15). Hatched areas are regions where (15) cannot be met. The one-layer, reduced gravity model is applicable in the remaining regions away from their boundaries.

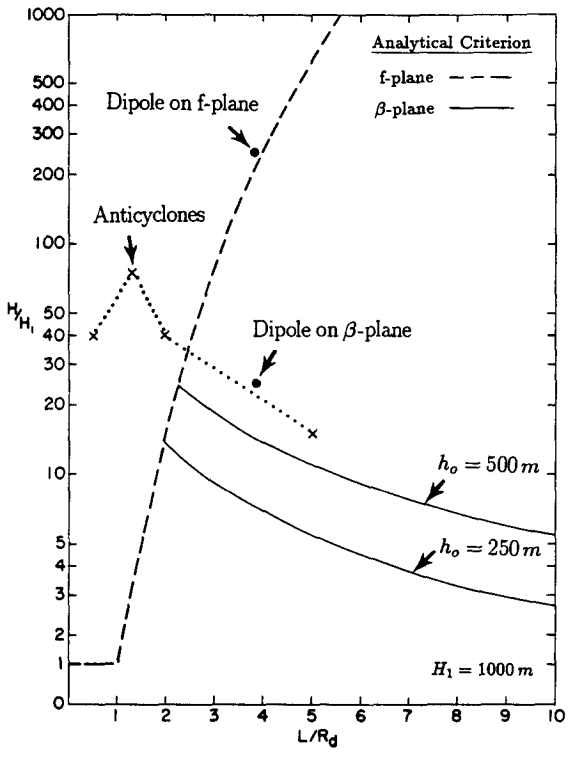

FIG. 12. Criterion (17) is satisfied when H/H_1 is much greater than the corresponding point on the dashed curve when on the f-plane and the minimum of the dashed and solid curve when on the β-plane. Crosses and dots are estimates of H^*/H_1 from the numerical experiments.

terion (17) is illustrated by a simple analysis of Phillips' model as performed by Pedlosky (1987). In the absence of β, the two-layer model will be baroclinically stable if

$$L < \pi f_o^{-1}[g'(H_1H_2)^{1/2}]^{1/2}$$

where L is the characteristic length scale of the disturbance (Pedlosky 1987). This implies as criterion (18) that

$$H_2 > \pi^2 H_1 \frac{L^4}{R_d^4} \quad \text{or} \quad H \gg H_1 \frac{L^4}{R_d^4}.$$

On the other hand, in the presence of β and with the flow mostly confined in the upper layer, the model will be baroclinically stable only if the vertical shear between the two layers is less than the critical value $\beta g' H_2/f_o$ (Pedlosky 1987). If one consider a relatively thick lower-layer with small velocities, then this condition is equivalent to

$$\frac{f_o}{g'}\frac{h_o}{L} < \frac{\beta g' H_2}{f_o} \quad \text{or} \quad H > h_o \frac{L_\beta}{L}$$

which is the contribution from the β-effect to criterion (17). Hence, it can be stated that the reduced-gravity model loses its validity when baroclinic instability processes must be retained.

In a study of waves and instabilities along fronts in a two-layer system, Killworth et al. (1984) (single-front) and Paldor and Killworth (1987) (double-front) examined how the presence of the second moving layer destabilizes the frontal waves. In the former study, all waves become stable when the lower-layer depth approaches infinity, while in the latter at least one wave does not. However, in either case, the asymptotic behavior is none other than that of the corresponding reduced-gravity model, whether stable or not. With the shortest length scale in the model being the frontal width (about the deformation radius), and with no β-effect, the criterion of the present theory reduces to $H \gg H_1$ in agreement with the results of the above studies.

4. Comparison with the analytical criterion

We are now in position to compare the analytical criterion (17) with the numerical simulations of section 2. For the parameter range of the described cyclones and anticyclones (H_1 = 1000 m, h_o = 500 m, L = 60 km), we have $\epsilon \sim 0.1$, $s \sim 0.2$ and $\beta = 1.2 \times 10^{-2}$, which satisfy the initial requirements of the scaling analysis. In this case, criterion (17) then states that the lower layer will be dynamically negligible if the total depth H satisfies

$$H \gg 3 \text{ km}.$$

This is consistent with the findings of section 2c, which show that it is only when H is greater than 50 km that we observe a negligible influence of the lower layer thickness on the dynamics of the upper layer ring (Fig. 2). With this set of parameters, in order for the reduced-gravity model to be valid, the lower layer must then be significantly deep and in any case much deeper than the real ocean depth. In other words, barotropic effects and baroclinic instability must be retained when considering eddies with the above scales.

The previous result was derived for only one set of parameters. Hence, in order to check the validity of analytical criterion (17), one has to perform a few more experiments. By keeping the Rossby deformation radius (R_d) and the initial interface displacement (h_o) constant, criterion (17) can be expressed as a function of the ring length scale over the internal Rossby radius of deformation, L/R_d:

$$\frac{H}{H_1} \gg \max\left[1, \min\left(\frac{L^4}{R_d^4}, K\frac{R_d}{L}\right)\right] \qquad (19)$$

where K is a constant equal to $h_o f_o/\beta_o R_d$. This expression is represented in Fig. 12 and, as presented in section 3, for $L > R_d$, is a combination of two curves resulting from f-plane dynamics (barotropic motions and baroclinic instabilities) and a contribution from the β-effect, respectively. The impact of the lower layer on the dynamics of the upper is the strongest when the

two curves intersect. In order to test expression (19), a series of experiments were performed with anticyclones of length scales, L, equal to $0.5R_d$, $1.3R_d$, $2R_d$ and $5R_d$, respectively.

At this point, one has to define a criterion to determine from the numerical experiments the minimum depth, H^*, for which the lower layer has a minimal influence on the upper-layer eddy. First, the experiment with ratio $\delta = 1/1000$ is considered to be equivalent to one with an infinitely deep lower layer. Then, H^* is defined as the minimum depth for which the westward drift of the upper-layer ring does not differ by more than 5% from the drift of the reference experiment ($\delta = 1/1000$). One could define a different H^* based on other assumptions, but the westward drift is felt to be a good characteristic of the eddy evolution.

The values of H^* for the above length scales, L, are represented by crosses in Fig. 12. Their distribution appears to follow the curves with allowance made for the strong inequality in (17), except that the maximum is not located where expected. We may recall that the criterion has been derived with a scaling analysis and, therefore, gives only an order of magnitude for both horizontal and vertical scales.

To further check the validity of the criterion, one can investigate the particular case of an f-plane. Since (17) reduces to (18) when $\beta_o = 0$, the lower-layer will always have a significant impact on the upper-layer dynamics if the length scale, L, is several Rossby deformation radii, R_d (Fig. 12). This point is clearly illustrated by a series of experiments initialized with a dipole on both the f- and β-planes. The dipole has been chosen in order to have a structure that evolves significantly through self-advection on an f-plane (which is not the case for an isolated eddy). The dipole is defined as

$$h = H_1 + h_o \frac{y}{L_o} e^{1/2} e^{-r^2/2L_o^2}$$

where $h_o = 250$ m and $L_o = 250$ km. The values of H_1, g', f_o and β_o are unchanged. This yields, according to Cushman-Roisin and Tang (1990), a length scale $L = (\sqrt{2}/2)L_o \sim 4R_d$ and criterion (17) becomes, on the β-plane

$$H \gg 7 \text{ km}$$

while, on the f-plane

$$H \gg 228 \text{ km}$$

which gives a clear ratio of 30 to 1 (Fig. 12). We should then observe a significant difference of behavior between the two experiments (f- or β-plane). This is indeed the case since, on the β-plane, the above dipole is found to have an $H^* \sim 25$ km while on an f-plane, $H^* \sim 250$ km (Fig. 12). Moreover, on the β-plane the westward drift of the dipole varies by only 0.6% between the ratios $\delta = 1/50$ and $\delta = 1/1000$, while on the f-plane the variation is 26%. Also of interest is the fact that, on the β-plane the dipole slows down as the lower-layer thickness decreases while the tendency is opposite on the f-plane.

Both series of experiments (eddies and dipoles) provided a wide range of parameters over which criterion (17) was tested. The theoretical predictions are in agreement with the numerical findings, and it can be concluded that the theory has led to a practical criterion.

5. Summary and conclusions

The validity of the reduced-gravity model (one active layer over another infinite and at rest), an approximation widely used to study the evolution of isolated vortices, has been investigated in detail with a primitive-equation, isopycnic-coordinate, two-layer numerical model whose upper-to-lower layer depth ratio was varied from 1/5 to 1/1000. The numerical findings were then compared to a scaling analysis of a two-layer system, which determined the conditions needed for the lower layer to have a negligible influence on the dynamics of the upper layer.

The scaling was performed with an emphasis on the geostrophic regimes (small Rossby number) which dominate oceanic features such as rings, but is also applicable to fully ageostrophic regimes. The derivation yielded the following criterion:

$$H \gg \max\left[H_1, \min\left(H_1 \frac{L^4}{R_d^4}, h_o \frac{L_\beta}{L}\right)\right]$$

where H, H_1, h_o, L, R_d and L_β are the total depth, the upper-layer depth, the interfacial displacement, the eddy length scale, the Rossby radius of deformation and the planetary scale, respectively.

The present numerical simulations confirm, as earlier models have shown, that nonlinear eddies in a finite depth ocean propagate at a nearly uniform rate while gradually decaying through the radiation of Rossby waves. Both a form drag exerted by the lower layer and interactions with the Rossby wave wake affect the migration and induce a meridional drift. This is consistent with the idea that, due to the energy loss by Rossby-wave radiation, eddies will tend to approach their so-called "latitude of rest". In the case of lenses (eddies whose isopycnals surface), the westward propagation speed does not vary as the ratio $\delta = h_o/H$ is varied and no appreciable meridional motion is observed, as long as the lens is stable (small δ). As $\delta = H_1/H$ decreases, cyclones and anticyclones (eddies whose undisturbed depth does not vanish along their rim) have the tendency to move westward faster and less meridionally. As the thickness of the lower layer increases, the meridional displacement decreases due to a smaller form drag of the lower layer. The only factor for the meridional displacement that remains in the case of a small

δ is the interactions with the Rossby wave wake. If this effect is suppressed, the ring should move purely westward, which is effectively the case with a lens. As the ratio δ increases, the coupling between the two layers intensifies and, for both lenses and cyclones, generate baroclinic instabilities.

Series of experiments over a wide range of parameters were performed to test the above criterion, and a minimum depth was defined from the numerical experiments for which the lower layer has a minimal influence on the upper-layer eddy. It was found that the theoretical predictions are in agreement with the numerical findings. A final set of experiments with dipoles on both the f- and β-planes clearly illustrated the two sides of the criterion and it was concluded that the theory performs as expected. In order for the reduced-gravity model to be valid, the total depth of fluid must be much larger than either of two values. These two values, resulting from f- and β-planes dynamics, apply to shorter and larger scales, respectively. At horizontal scales up to the deformation radius, a lower layer much deeper (by a factor of ten or so) than the upper layer is sufficient. For increasing length scales beyond the deformation radius, on both the f- and β-planes, the reduced-gravity model rapidly loses its validity. The model recovers its validity toward larger scales on the β-plane.

For mesoscale features such as rings, the lower layer must be significantly deep and in any case much deeper than the real ocean depth. In other words, processes such as barotropic motion and baroclinic instability must be retained. One can also expect that, in the presence of topography and/or ambient shear, the criterion will include additional terms which may enlarge or further restrict the validity of the reduced-gravity model.

Acknowledgments. The authors wish to thank Dr. Nof for helpful comments. In particular, E. P. C. appreciated his hospitality during his stay at Florida State University. Conversations with D. Boudra, P. Cessi, W. Dewar, D. Olson, C. Rooth, M. Stern and, especially G. Flierl, proved timely and valuable. Support was provided by the Office of Naval Research through Grant N00014-89-J-1574 and N00014-89-J-1606 and by the National Science Foundation through Grant OCE-8711030. The computations were carried out using the CRAY-XMP at the National Center for Atmospheric Research. NCAR is sponsored by the National Science Foundation.

APPENDIX A

Determination of the Coefficients ω and γ

Nondimensionalization of Eqs. (8) yields

$$p_1 = \eta + \gamma\pi, \quad p_2 = \pi, \tag{20}$$

while nondimensionalization of the momentum equations (5–6) provides for each layer:

$$\omega u_{1t} + \epsilon(u_1 u_{1x} + v_1 u_{1y}) - v_1 - \beta y v_1 = -p_{1x} \tag{21}$$

$$\omega v_{1t} + \epsilon(u_1 v_{1x} + v_1 v_{1y}) + u_1 + \beta y u_1 = -p_{1y} \tag{22}$$

$$\omega u_{2t} + \gamma\epsilon(u_2 u_{2x} + v_2 u_{2y}) - v_2 - \beta y v_2 = -p_{2x} \tag{23}$$

$$\omega v_{2t} + \gamma\epsilon(u_2 v_{2x} + v_2 v_{2y}) + u_2 + \beta y u_2 = -p_{2y} \tag{24}$$

With ω, ϵ, $\gamma\epsilon$ and β all much less than unity, the leading-order balances of the above equations correspond to f-plane geostrophic equilibrium, i.e., $u_i = -p_{iy}$, $v_i = p_{ix}$. Replacing the velocities by these first-order expressions in the small terms yields to the next order of approximation:

$$u_1 = -p_{1y} - \omega p_{1xt} - \epsilon J(p_1, p_{1x}) + \beta y p_{1y} \tag{25}$$

$$v_1 = +p_{1x} - \omega p_{1yt} - \epsilon J(p_1, p_{1y}) - \beta y p_{1x} \tag{26}$$

$$u_2 = -p_{2y} - \omega p_{2xt} - \gamma\epsilon J(p_2, p_{2x}) + \beta y p_{2y} \tag{27}$$

$$v_2 = +p_{2x} - \omega p_{2yt} - \gamma\epsilon J(p_2, p_{2y}) - \beta y p_{2x}. \tag{28}$$

After nondimensionalization, the continuity equation (7) for the upper layer can be written as

$$\omega\eta_t + \epsilon(u_1\eta_x + v_1\eta_y) + (s + \epsilon\eta)(u_{1x} + v_{1y}) = 0, \tag{29}$$

which, after replacement of u_1 and v_1 by (25)–(26), replacement of p_1 by (20), and neglect of terms of higher order, becomes

$$\omega\frac{\partial}{\partial t}(s\nabla^2\eta + s\gamma\nabla^2\pi - \eta) - \gamma\epsilon J(\pi, \eta) + s\epsilon J(\eta + \gamma\pi, \nabla^2\eta + \gamma\nabla^2\pi) + \epsilon^2 J(\eta, \eta\nabla^2\eta + \frac{1}{2}\nabla\eta\cdot\nabla\eta) + s\beta(\eta_x + \gamma\pi_x) + \beta\epsilon\eta\eta_x = 0. \tag{30}$$

The last equation can be interpreted as a sum of prognostic and diagnostic terms (those with and without a time derivative, respectively). The prognostic terms provide the rate at which variables will evolve from any imbalance among the diagnostic terms. Hence, it is reasonable to state that the system chooses its own time scale (dimensionless number ω) such that the leading prognostic term in (30) is of the same order as the leading diagnostic term.

Mathematically, this statement implies

$$\max(s\omega, s\gamma\omega, \omega) = \max(\gamma\epsilon, s\epsilon, s\gamma\epsilon, s\gamma^2\epsilon, \epsilon^2, s\beta, s\beta\gamma, \beta\epsilon),$$

or, since $\gamma \leqslant 1$ and $\epsilon \leqslant s$,

$$\omega = \frac{\max(\gamma\epsilon, s\epsilon, s\beta)}{\max(s, 1)}. \tag{31}$$

The dominant terms in the lower-layer continuity equation are identical (but with opposite signs) to the dominant terms of the upper-layer continuity equation. Hence, to obtain an independent equation at the leading order, one must formulate the sum of these equations, namely the continuity equation for the entire

system. Adding Eq. (7) for each layer and replacing h_1 and h_2 by (9), one obtains

$$[(u_1 - u_2)\eta_x + (v_1 - v_2)\eta_y] + (H_1 + \eta)[(u_1 - u_2)_x + (v_1 - v_2)_y] + H(u_{2x} + v_{2y}) = 0, \quad (32)$$

which after nondimensionalization becomes

$$\epsilon[(u_1 - \gamma u_2)\eta_x + (v_1 - \gamma v_2)\eta_y] + (s + \epsilon\eta)[(u_1 - \gamma u_2)_x + (v_1 - \gamma v_2)_y] + \frac{s\gamma}{\delta}(u_{2x} + v_{2y}) = 0. \quad (33)$$

Replacement of the velocity components by their expressions (25–28) and then of the pressures by expressions (20) yields

$$\frac{s\gamma\omega}{\delta}\nabla^2\pi_t + s\omega\nabla^2\eta_t + \epsilon\omega\nabla\cdot(\eta\nabla\eta_t) + s\epsilon J(\eta, \nabla^2\eta) + \epsilon^2 J(\eta, \eta\nabla^2\eta + \tfrac{1}{2}\nabla\eta\cdot\nabla\eta) + s\gamma\epsilon[J(\pi, \nabla^2\eta) + J(\eta, \nabla^2\pi)] + \gamma\epsilon^2[\eta J(\pi, \nabla^2\eta) + \eta J(\eta, \nabla^2\pi) + J(\pi, \nabla\eta)\cdot\nabla\eta + J(\eta, \nabla\pi)\cdot\nabla\eta] + \frac{s\gamma^2\epsilon}{\delta}J(\pi, \nabla^2\pi) + s\beta\eta_x + \beta\epsilon\eta\eta_x + \frac{s\beta\gamma}{\delta}\pi_x = 0. \quad (34)$$

Since the above equation corresponds to a property integrated over the entire depth of the system, namely continuity of volume, it is logical to interpret it as an equation governing the barotropic component of the flow field. Hence, Eq. (34) will be used to establish the order of magnitude of π, which after scaling amounts to the determination of the dimensionless number γ measuring the relative amplitude of the barotropic flow. As for the determination of ω, we equate the largest term containing γ to the largest term not containing γ, or

$$\max\left(\frac{s\gamma\omega}{\delta}, s\gamma\epsilon, \gamma\epsilon^2, \frac{s\gamma^2\epsilon}{\delta}, \frac{s\beta\gamma}{\delta}\right) = \max(s\omega, \epsilon\omega, s\epsilon, \epsilon^2, s\beta, \beta\epsilon).$$

Again, since $\gamma \leqslant 1$ and $\epsilon \leqslant s$, this can be simplified to

$$\gamma = \delta\frac{\max(\omega, \epsilon, \beta)}{\max(\omega, \delta\epsilon, \gamma\epsilon, \beta)}. \quad (35)$$

Equations (31) and (35) are the two coupled equations that provide the secondary dimensionless numbers ω and γ. One now proceeds with the solution of these equations. First, one notes that the term $\delta\epsilon$ in the denominator of (35) can be dropped. Indeed, if this term were the largest, i.e., if $\delta\epsilon > \max(\omega, \gamma\epsilon, \beta)$, the $\gamma = \delta\max(\omega, \epsilon, \beta)/\delta\epsilon$ or $\gamma\epsilon = \max(\omega, \epsilon, \beta)$, from which follows $\delta\epsilon > \max(\omega, \max(\omega, \epsilon, \beta), \beta) = \max(\omega, \epsilon, \beta) \geqslant \epsilon$. Hence, this hypothesis leads to $\delta\epsilon > \epsilon$ or $\delta > 1$, which is contrary to our starting assumption. Hence $\delta\epsilon \leqslant \max(\omega, \gamma\epsilon, \beta)$, and (35) can be simplified to

$$\gamma = \delta\frac{\max(\omega, \epsilon, \beta)}{\max(\omega, \gamma\epsilon, \beta)}. \quad (36)$$

At this stage, it becomes convenient to distinguish between two cases, that of length scales shorter than or equal to the deformation radius ($s \geqslant 1$) and that of longer length scales ($s < 1$). For $s \geqslant 1$, (31) yields $\omega = \max(\gamma\epsilon/s, \epsilon, \beta) = \max(\epsilon, \beta)$ since $\gamma \leqslant 1$ and $1/s \leqslant 1$. Substitution of this solution for ω into (36) provides $\gamma = \delta$, i.e., the pressure ratio is identical to the depth ratio.

For longer length scales, $s < 1$, (31) yields $\omega = \max(\gamma\epsilon, s\epsilon, s\beta)$ and substitution into (36) provides

$$\gamma = \delta\frac{\max(\epsilon, \beta)}{\max(s\epsilon, \gamma\epsilon, \beta)}.$$

APPENDIX B

The Ageostrophic Case

When the Rossby number is unity ($\epsilon = 1$), the barotropic equation (33) yields, without approximation, terms on the order of 1, γ, s, $s\gamma$ and $s\gamma/\delta$, where the γ-terms represent the contributions of the lower-layer velocity components. The balance of this equation requires

$$\max\left(\gamma, s\gamma, \frac{s\gamma}{\delta}\right) = \max(1, s).$$

Now, since $\delta < 1$ and $1 = \epsilon \leqslant s$ [from inequalities (10) which still hold in the ageostrophic context], the above equality reduces to

$$\gamma = \delta,$$

which means that the pressures are again in the same ratio as the layer depths.

The presence of the lower layer is felt in the upper-layer primitive equations, (21)-(22)-(29), only via the pressure p_1, which is given by the hydrostatic balance (20): $p_1 = \eta + \gamma\pi$. Hence, the lower-layer has a negligible influence on the upper-layer dynamics if the contribution of π can be neglected in p_1, i.e., if $\gamma \ll 1$. This immediately leads to the criterion $\delta \ll 1$. As it turns out, criterion (16) applied under the present conditions, namely $\beta \ll 1 = \epsilon \leqslant s$, yields the same expression. Therefore, criterion (16) and its dimensional form (17), derived for geostrophic motions, also apply to ageostrophic motions.

Ageostrophic motions are naturally characterized by an inertial time scale ($\omega = 1$, in the present notation). Other, low-frequency motions, such as Rossby waves, that may occur concomitantly, are in near-geostrophic

balance and are thus governed by the previous analysis. For these, the full criterion (17) remains in force.

REFERENCES

Bleck, R., and D. B. Boudra, 1986: Wind-driven spin up in eddy-resolving ocean models formulated in isopycnic and isobaric coordinates. *J. Geophys. Res.*, **91,** 7611–7621.

Chassignet, E. P., 1989: On the meridional propagation of isolated eddies. GFD Summer Study Program. WHOI Tech. Rep. 89-54, 236–259.

——, and D. Nof, 1989: The propagation of isolated nonlinear eddies in a finite depth ocean. FSU Tech. Rep. 1-90, 29 pp.

——, D. B. Olson and D. B. Boudra, 1990: Motion and evolution of oceanic rings in a numerical model and in observations. *J. Geophys. Res.*, in press.

Cushman-Roisin, B., 1986: Frontal geostrophic dynamics. *J. Phys. Oceanogr.*, **16,** 132–143.

——, and B. Tang, 1990: Geostrophic turbulence and emergence of eddies beyond the radius of deformation. *J. Phys. Oceanogr.*, **20,** 97–113.

——, E. P. Chassignet and B. Tang, 1990: Westward motion of mesoscale eddies. *J. Phys. Oceanogr.*, **20,** 758–768.

Davey, M. K., and P. D. Killworth, 1984: Isolated waves and eddies in a shallow water model. *J. Phys. Oceanogr.*, **14,** 1047–1064.

Flierl, G. R., 1977: The application of linear quasigeostrophic dynamics to Gulf Stream rings. *J. Phys. Oceanogr.*, **7,** 365–379.

——, 1984: Rossby wave radiation from a strongly nonlinear warm eddy. *J. Phys. Oceanogr.*, **14,** 47–58.

——, 1987: Isolated eddy models in geophysics. *Ann. Rev. Fluid Mech.*, **19,** 493–530.

Iselin, C. O., 1939: The influence of vertical and lateral turbulence on the characteristics of the waters at mid-depth. *Trans. Amer. Geophys. Union,* **20,** 414–417.

Kamenkovich, V. M., M. N. Koshlyakov and A. S. Monin, 1986: *Synoptic Eddies in the Ocean.* D. Reidel, 433 pp.

Killworth, P. D., 1983: On the motion of isolated lenses on a beta-plane. *J. Phys. Oceanogr.*, **13,** 368–376.

——, N. Paldor and M. E. Stern, 1984: Wave propagation and growth on a surface front in a two-layer geostrophic current. *J. Mar. Res.*, **42,** 761–785.

Larichev, V. D., 1983: General properties of nonlinear synoptic dynamics in the simplest model of barotropic ocean. *Oceanologiya,* **23,** 551–558.

McWilliams, J. C., 1989: Geostrophic vortices. *Proceedings International School of Physics "Enrico Fermi".* Italian Physical Society, in press.

——, and G. R. Flierl, 1979: On the evolution of isolated non-linear vortices, with application to Gulf Stream rings. *J. Phys. Oceanogr.*, **9,** 1155–1182.

——, P. R. Gent and N. J. Norton, 1986: The evolution of balanced, low-mode vortices on the β-plane. *J. Phys. Oceanogr.*, **16,** 838–855.

Matsuura, T., and T. Yamagata, 1982: On the evolution of nonlinear planetary eddies larger than the radius of deformation. *J. Phys. Oceanogr.*, **12,** 440–456.

Mied, R. P., and G. J. Lindemann, 1979: The propagation and evolution of cyclonic Gulf Stream rings. *J. Phys. Oceanogr.*, **9,** 1183–1206.

Montgomery, R. B., 1940: The present evidence on the importance of lateral mixing processes in the ocean. *Bull. Amer. Meteor. Soc.*, **21,** 87–94.

Nof, D., 1981: On the β-induced movement of isolated baroclinic eddies. *J. Phys. Oceanogr.*, **11,** 1662–1672.

——, 1983a: On the migration of isolated eddies with application to Gulf Stream rings. *J. Mar. Res.*, **41,** 399–425.

——, 1983b: The translation of isolated cold eddies on a sloping bottom. *Deep-Sea Res.*, **30,** 171–182.

Norton, N. J., J. C. McWilliams and P. R. Gent, 1986: A numerical model of the Balance Equations in a periodic domain and an example of balanced turbulence. *J. Comput. Phys.*, **67,** 439–471.

Olson, D. B., 1980: The physical oceanography of two rings observed by the cyclonic ring experiment. II: Dynamics. *J. Phys. Oceanogr.*, **10,** 514–528.

——, and R. H. Evans, 1986: Rings of the Agulhas. *Deep-Sea Res.*, **33,** 27–42.

——, R. W. Schmitt, M. Kennelly and T. M. Joyce, 1985: A two-layer diagnostic model of the long-term physical evolution of warm-core ring 82B. *J. Geophys. Res.*, **90,** 8813–8822.

Paldor, N., and P. D. Killworth, 1987: Instabilities of a two-layer coupled front. *Deep-Sea Res.*, **34,** 1525–1539.

Pedlosky, J., 1987: *Geophysical Fluid Dynamics,* second ed. Springer-Verlag, 624 pp.

Polvani, L. M., N. J. Zabusky and G. R. Flierl, 1989: Two-layer geostrophic vortex dynamics. Part 1. Upper-layer V-states and mergers. *J. Fluid Mech.*, **205,** 215–242.

Ripa, P., 1989: On the stability of ocean vortices. *Mesoscale/Synoptic Coherent Structures in Geophysical Turbulence.* Nihoul and Jamart, Eds., Elsevier Oceanogr. Ser., **50,** 167–179.

Smith, D. C., and R. O. Reid, 1982: A numerical study of nonfrictional decay of mesoscale eddies. *J. Phys. Oceanogr.*, **12,** 244–255.

Williams, G. P., and T. Yamagata, 1984: Geostrophic regimes, intermediate solitary vortices and Jovian eddies. *J. Atmos. Sci.*, **41,** 453–478.